CPC(HEP & NP), 2009, **33**(6): 481—486 Chinese Physics C Vol. 33, No. 6, Jun., 2009

Rapidity dependence of hadron p_T spectra in central Au+Au collisions at $\sqrt{s_{NN}}=200$ GeV*

SHAO Feng-Lan(邵凤兰)[1;1)] SONG Jun(宋军)[2] XIE Qu-Bing(谢去病)[2;2)]

1 (Department of Physics, Qufu Normal University, Qufu 273165, China)
2 (Department of Physics, Shandong University, Ji'nan 250100, China)

Abstract The transverse momentum spectra for identified hadrons at different rapidities in central Au+Au collisions at $\sqrt{s_{NN}}=200$ GeV are studied in a quark combination model. The results for p_T spectra of $\pi^{\pm}$, $K^{\pm}$, $p(\overline{p})$ and for the p/π ratios in a broader p_T range at midrapidity agree well with the data. The transverse momentum spectra of pions, protons and antiprotons at various rapidities $y\sim 1$, $\eta=2.2$ and $y\approx 3.2$ are calculated and compared with the data.

Key words relativistic heavy ion collisions, hadronization, quark combination

PACS 25.75.Dw, 25.75.-q

1 Introduction

The relativistic heavy ion collider (RHIC) at Brookhaven National Lab (BNL) provides a unique environment to search for the quark gluon plasma (QGP) predicted by lattice QCD calculations[1], and to study the properties of this matter at extremely high energy densities. A huge number of data have been accumulated and used to extract the information about the original partonic system and its space-time evolution. A variety of experimental facts from various aspects imply that the strongly coupled QGP has been probably produced in central Au+Au collisions at RHIC[2—7]. Due to the confinement effects, one can only detect the hadrons frozen out from the partonic system rather than directly detect the partons produced in the collisions. Therefore, one of the important prerequisites for exploring the quark gluon plasma is the better understanding of the hadronization mechanism in nucleus-nucleus collisions.

The quark combination picture is successful in describing many features of multi-particle production in high energy collisions. The parton coalescence and recombination models have explained many highlights at RHIC, such as the high ratio of p/π at intermediate transverse momenta[8—10] and the quark number scaling of hadron elliptic flows[11—13]. Our quark combination model has described the charged particle pseudorapidity densities[14], hadron multiplicity ratios, p_T spectra[15] and elliptic flows [16] at midrapidity.

Recently the STAR collaboration has finely measured the transverse spectra for identified baryons and mesons in a wider transverse momentum range in central Au+Au collisions at $\sqrt{s_{NN}}=200$ GeV[17]. The BRAHMS collaboration has given the transverse momentum distributions for identified hadrons at different rapidities[18—20]. It provides a good opportunity to study the hadron production mechanism in a larger transverse momentum range and at different rapidities. In this paper, we use our quark combination model to study the transverse momentum distributions for identified hadrons at different rapidities $y\sim 0,1$, $\eta=2.2$ and $y\approx 3.2$ in central Au+Au collisions at $\sqrt{s_{NN}}=200$ GeV.

Received 24 July 2008
* Supported by National Natural Science Foundation of China (10775089, 10475049) and Science Fund of Qufu Normal University

1) E-mail: shaofl@mail.sdu.edu.cn
2) E-mail: xie@sdu.edu.cn

2 A brief introduction of the quark combination model

In this section we give a brief description of our quark combination model. The model was first proposed for high energy e^+e^- and pp collisions[21—26]. It has also been applied to the multi-parton systems in high energy e^+e^- annihilations[27—30]. Recently we have extended the model to ultra-relativistic heavy ion collisions[14—16].

The quark production from vacuum is a very sophisticated nonperturbative process. We have developed a simple model for quark production that is of statistical nature without dynamic details in e^+e^- collisions[21]. It has been found in the PHOBOS experiments that in the energy range $\sqrt{s_{\rm NN}} \approx$ 20—200 GeV, the total multiplicity per participating nucleon pair $(\langle N_{\rm ch}\rangle/\langle N_{\rm part}\rangle)$ in central Au+Au collisions scales with $\sqrt{s_{\rm NN}}$ in the same way as $\langle N_{\rm ch}\rangle$ with $\sqrt{s}$ in e^+e^- collisions[31]. In addition, the same effect has also been observed in pp and $p\overline{p}$ data after correcting the leading particle effect[31]. This suggests a universal mechanism for particle production in strongly interacting systems at high energies, which is mainly controlled by the amount of effective energy available (per participant pair for heavy ion collisions). Based on these experimental facts we have extended the model to nucleus nucleus collisions at RHIC energy in Ref. [14].

Our quark combination model describes the hadronization production of initially produced ground state mesons (36-plets) and baryons (56-plets). In principle the model can also be applied to the production of excited states[23]. These hadrons, through combinations of the constituent quarks, are then allowed to decay into the final state hadrons. We take into account the decay contributions of all resonances of 56-plets baryons and 36-plets mesons, and cover all available decay channels by using the decay program of PYTHIA 6.1[32]. The main idea is to line up $N_{\rm q}$ quarks and anti-quarks in a one-dimensional order in phase space, e.g. in rapidity, and let them combine into the initial hadrons one by one following a combination rule. See section 2 of Ref. [15] for short description of such a rule. Of course, we also take into account the near correlation in transverse momentum by limiting the maximum transverse momentum difference $\Delta p_{\rm T}$ for quarks and antiquarks as they combine into hadrons. We note that it is very straightforward to define the combinations in one dimensional phase space, but it is highly complicated to do it in two or three dimensional phase space[33]. The flavor $SU(3)$ symmetry with strangeness suppression in the yields of initially produced hadrons is fulfilled in the model[21, 23].

3 Transverse distributions of quarks and antiquarks

The main purpose of the paper is to study the applicability of the quark combination mechanism in a wider transverse momentum regions and at different rapidities. Firstly, we have to know the momentum distribution of light and strange quarks and antiquarks just before hadronization. It is known that the relativistic hydrodynamic description of the evolution for the thermal parton matter produced in nucleus-nucleus collisions is in many aspects successful. This provides impressive evidence that the bulk of the partonic matter produced in collisions shows efficient thermalization and behaves hydrodynamically. What we need is only the momentum distribution of quarks at the point of hadronization rather than its time evolution. When the expansive thermal medium evolves to the point of the hadronization, the momentum distributions of quarks and antiquarks can be described by a thermal phenomenology proposed in Ref. [34].

Taken into account the transverse flow of the thermal medium, the quarks and antiquarks get a transverse boost described by a flow velocity profile $\beta_r(r)$ as a function of transverse radial positions r. $\beta_r(r)$ is parameterized by the surface velocity β_s: $\beta_r(r)=\beta_s\,(r/R_{\max})^n$. The transverse flow of the thermal medium can be equivalently described by a superposition of a set of thermal sources, each boosted with a transverse rapidity $\rho=\tanh^{-1}\beta_r$[34]

$$\frac{{\rm d}n_{\rm th}}{2\pi p_{\rm T}{\rm d}p_{\rm T}} = N\int_0^{R_{\max}} r\,{\rm d}r\,m_{\rm T}\times I_0\left(\frac{p_{\rm T}\sinh\rho}{T}\right)K_1\left(\frac{m_{\rm T}\cosh\rho}{T}\right), \quad (1)$$

where I_0 and K_1 are modified Bessel functions. N is the normalization constant. The value of $R_{\max}$ is taken to be $R_{\max}=13$ fm[35]. The hadronization temperature T is taken to be 170 MeV. Values of the parameters n, $\beta_{\rm s}$ for light and strange quarks and antiquarks are extracted from the transverse momentum distributions of π^0 and $K^0_{\rm s}$ at midrapidity in our quark combination model.

The quarks and antiquarks with high transverse momenta come mainly from the minijets created in the initial hard collisions among nucleons. By initial hard scattering partons that initiate minijets acquire a large transverse momentum. Subsequently they further evolve by gluon radiation and conversion of gluons to quark and antiquark pairs until hadronization. The evolution is accompanied by the loss of momenta and virtuality for hard partons. In the quark combination picture, the initial hard partons after hard scattering are not immediately ready for combination. What we consider is the combination of quarks and antiquarks just before hadronization. Those quarks and antiquarks are the parton remnants after the evolution of the initial hard partons by gluon radiation and gluon split. They are different from the jet initiating hard partons that fragment into hadrons in the fragmentation model. The large p_T spectra of identified hadrons measured by RHIC experiments exhibit a power-law behavior[17, 36]. Considering the parton-hadron duality, the transverse momentum distribution of minijet quarks should also have a power-law behavior. It can be parameterized as

$$\frac{\mathrm{d}n_{\mathrm{jet}}}{2\pi p_T \mathrm{d}p_T} = A\left(\frac{B}{B+p_T}\right)^C. \tag{2}$$

For thermal quarks, We take $n = 0.5$ for light and strange quarks and antiquarks, $\beta_s = 0.45c$, $0.56c$ for light and strange quarks/antiquarks, respectively. Values of the parameters A, B and C for minijet quarks are given in Table 1. Normalized transverse momentum distributions for light and strange quarks and antiquarks at midrapidity in central Au+Au collisions at $\sqrt{s_{NN}}=200$ GeV are shown in Fig. 1.

Table 1. Parameters for minijet quark distributions given in Eq. (2) at midrapidity in central Au+Au collisions at $\sqrt{s_{NN}}=200$ GeV.

	A/GeV^{-2}	B/GeV^{-1}	C
$u,\bar{u}$ and $d,\bar{d}$	2.32	1.5	7.25
$s,\bar{s}$	4.51	1.5	9.5

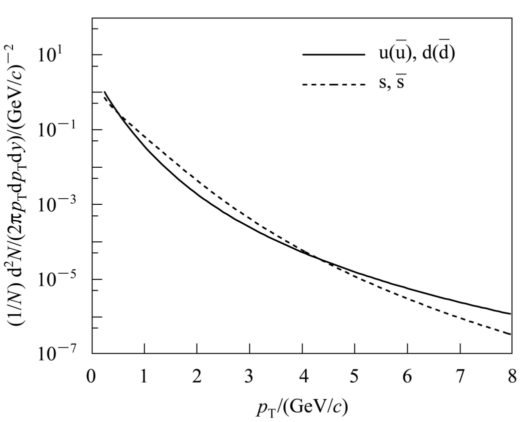

Fig. 1. Transverse momentum spectra of quarks and antiquarks at midrapidity just before hadronization in central Au+Au collisions at $\sqrt{s_{NN}}=200$ GeV.

4 Rapidity dependence of transverse momentum spectra for identified hadrons

In this section, we use our quark combination model to compute the transverse momentum spectra of identified hadrons at different rapidities. The total number of newborn quarks and antiquarks is given by our quark production model[14], and the number of net-quarks from colliding nucleons is three times of the number of participants. It has been found in STAR Collaboration experiments that the π^-/π^+ and $\bar{p}/p$ ratios as a function of p_T at midrapidity are almost constants within a broad transverse momentum region[17]. The transverse momentum distribution of

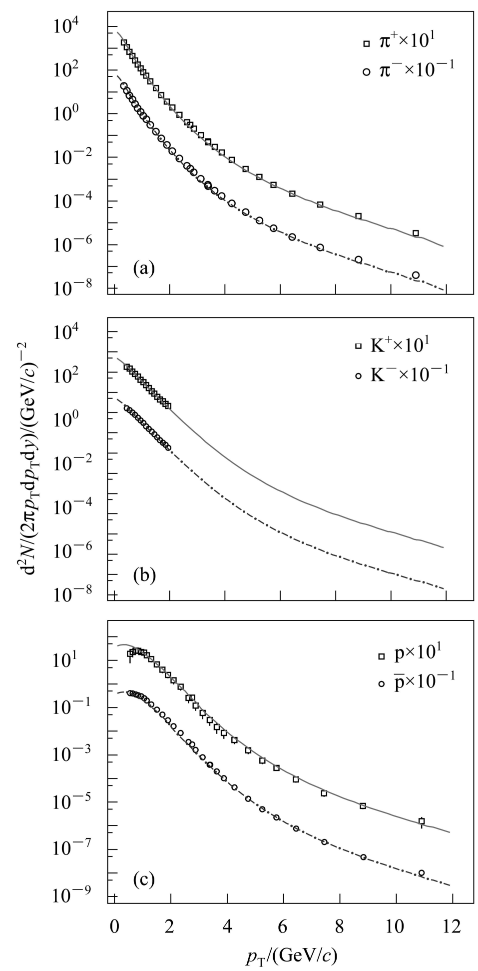

Fig. 2. Transverse momentum spectra of pions (a), kaons (b), proton and antiproton (c) at midrapidity in central Au+Au collisions at $\sqrt{s_{NN}} = 200$ GeV. The solid lines are our results for π^+, K^+ and p, and the dotted-dashed lines are for π^-, K^- and $\bar{p}$ respectively. The data of pions, proton and antiproton are from the STAR Collaboration[17], and kaons are from BRAHMS Collaboration[18].

net-quarks from colliding nucleons is taken the same as that of newborn light quarks at midrapidity. We use $\Delta p_{\mathrm{T}} = 0.66$ GeV for mesons and $\Delta p_{\mathrm{T}} = 1.0$ GeV for baryons, respectively. With this input, we can compute the transverse momentum distributions of various hadrons.

We calculate the transverse momentum spectra of pions, kaons, proton and antiproton at midrapidity in central Au+Au collisions at $\sqrt{s_{\mathrm{NN}}} = 200$ GeV. The results are shown in Fig. 2. The pions spectra are corrected to remove the feed-down contributions from $\mathrm{K}^0_{\mathrm{s}}$ and Λ. The feed-down contributions from Λ and Σ^+ are subtracted from the proton spectrum. Our quark combination model well explain the data in a large p_{T} range.

Recently the STAR Collaboration has measured the p/π^+ and $\overline{\mathrm{p}}/\pi^-$ ratios at large transverse momenta in central Au+Au collisions at $\sqrt{s_{\mathrm{NN}}} = 200$ GeV, and compared the data with the predictions of the recombination and coalescence models[17]. It is found that p/π^+ and $\overline{\mathrm{p}}/\pi^-$ ratios peak at $p_{\mathrm{T}} \sim$ 2—3 GeV with values close to unity, decrease with increasing p_{T}, and approach $\mathrm{p}/\pi^+ \approx 0.4$, $\overline{\mathrm{p}}/\pi^- \approx 0.25$ at $p_{\mathrm{T}} \gtrsim 7$ GeV. These models can qualitatively describe the $\mathrm{p}(\overline{\mathrm{p}})/\pi$ ratio at intermediate p_{T} but in general underpredict the results at high p_{T}[17]. We also compute the p/π^+ and $\overline{\mathrm{p}}/\pi^-$ ratios in the range $p_{\mathrm{T}} < 12$ GeV. The calculation results are shown in Fig. 3. Our results agree with the experimental data in the full p_{T} range.

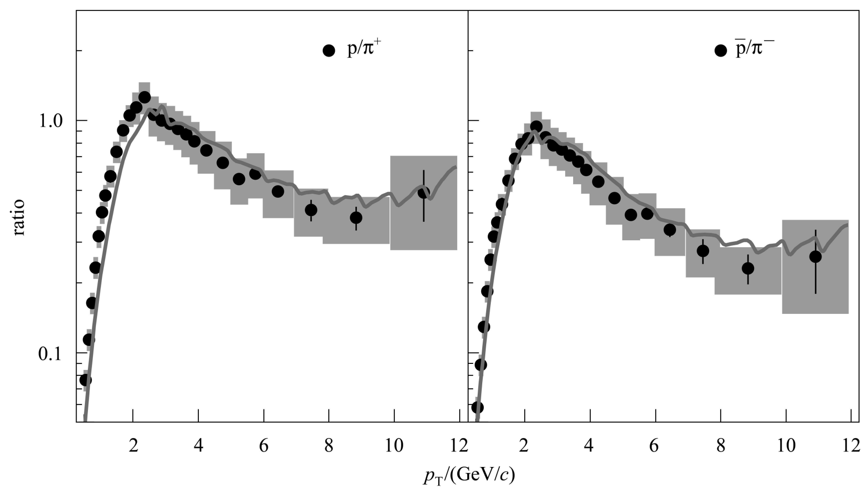

Fig. 3. The ratios of p/π^+ and $\overline{\mathrm{p}}/\pi^-$ as a function of transverse momentum at midrapidity in central Au+Au collisions at $\sqrt{s_{\mathrm{NN}}} = 200$ GeV. The shaded boxes represent the systematic uncertainties. The solid lines are our results. Experimental data are given by STAR Collaboration [17].

One can see from the above results that the quark combination model can reproduce the productions of identified hadrons quite well in a larger transverse momentum range. It suggests that the quark combination mechanism may still play an important role at high transverse momentum up to 12 GeV/c.

A variety of experimental facts at RHIC indicate that the QGP has been probably produced at midrapidity. Based on this indication the quark combination picture has successfully explained the hadron production at midrapidity[15, 37, 38]. However, can the QGP extend to forward rapidity? If it does, how much rapidity can it extend to? Can the combination picture describe the hadron production at forward rapidity yet? Fortunately, the BRAHMS Collaboration recently has measured the p_{T} spectra of identified hadrons at different rapidities[18—20]. It provides an opportunity to study the hadrons production at different rapidities and the rapidity dependence of hadron transverse momentum spectra. We now make a straightforward extension to the forward rapidity region, and this extension should be made with no change in the quarks p_{T} spectra before we draw some useful physical information from it.

We compute the transverse momentum spectra of pions and protons at $y \sim 1$ in central Au+Au collisions at $\sqrt{s_{\mathrm{NN}}} = 200$ GeV, the results are shown in Fig. 4(a). The proton and antiproton spectra are corrected to remove the feed-down contributions from Λ and $\overline{\Lambda}$ weak decays. No significant changes for the transverse spectra of pions and protons(antiprotons) are observed within one unit around midrapidity. It suggests that the hadron production at this rapidity is still dominated by combinations in the intermediate transverse momentum range. The QGP may still exist at $y \sim 1$ and it may extend much higher values than this rapidity.

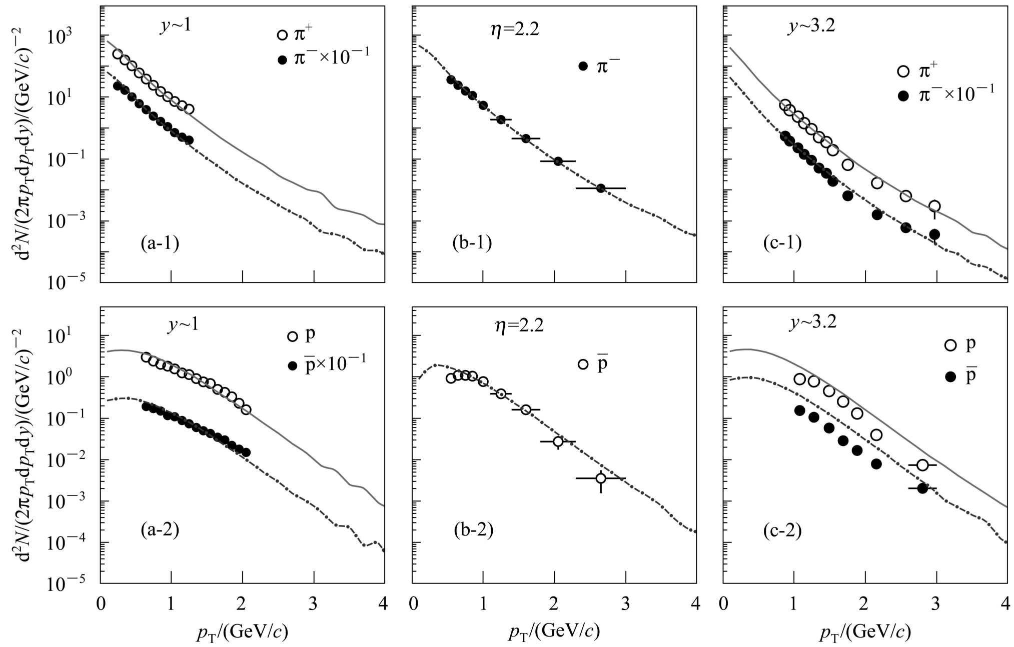

Fig. 4. Transverse momentum spectra of pions and protons at $y\sim1$ (a), $\eta=2.2$ (b) and $y=3.2$ (c) in central Au+Au collisions at $\sqrt{s_{NN}}=200$ GeV. The solid lines are our results for π^+ and p, and the dotted-dashed lines are for π^- and $\bar{p}$. The data of panel (a), (b), (c) are given by BRAHMS Collaboration[18—20].

In Fig. 4(b), we show the transverse momentum spectra of pions and antiprotons at $\eta=2.2(2.14<\eta<2.26)$ in central Au+Au collisions at $\sqrt{s_{NN}}=200$ GeV. The correction for feed-down from the (anti-) lambda decays has been applied, whereas the contamination of pions due to weak decays has not been corrected. Our model can also well describe the hadronic production at this rapidity.

We further compute the transverse spectra of pions and (anti-)protons at $y\approx3.2$, the results are shown in Fig. 4(c). No correction for decays or feed-down has been applied to the data. One can see that the computed results are in good agreement with the data for pions, but can not reproduce the data for protons and antiprotons. This is probably because the transverse momentum distribution of the net-quarks varies with rapidity in nucleus-nucleus collisions at RHIC. The amount of net-quarks is marginal compared with that of newborn quarks in the midrapidity region. Net-quarks may be highly thermalized due to interactions with newborn quarks. Its transverse momentum distribution will asymptotically tend to that of newborn light quarks. However the amount of net-quarks can approach and even exceed that of newborn quarks at large rapidity. Therefore the thermalization extent of net-quarks at large rapidity is much smaller than that at midrapidity. Its transverse momentum distribution at large rapidity may be obviously different from that of newborn quarks. It has been found that the yields and rapidity densities of protons and antiprotons are more sensitive to the existence of net-quarks than that of pions in the quark combination mechanism. Thus the rapidity dependence of the transverse momentum distribution for net-quarks should be mainly embodied by that of protons and antiprotons, rather than that of pions. It is one of the probable reasons why our quark combination model can describe well the data of pions, but less good those of protons and antiprotons at $y\approx3.2$.

From the above results, we can see that the quark combination model is able to describe the transverse momentum distribution of identified hadrons in a broad rapidity range $0<y<3.2$. This implies that the quark combination hadronization mechanism is still applicable to larger rapidities (at least $y=3.2$). On the other hand, the BRAHMS Collaboration has measured the nuclear modification factor R_{AA} for identified hadrons at forward rapidities in central Au+Au collisions at $\sqrt{s_{NN}}=200$ GeV[20], and the data also indicate the existence of the quark combination mechanism at forward rapidity. The continued suppression seen in the R_{AA} at $y=3.2$ further suggests that there is different physics from that at midrapidity. The absence of suppression in particle production at large transverse momentum in d+Au collisions shows that the suppression in central Au+Au collisions at midrapidity is not an initial-state effect but a final-state effect of the produced density medium (jet quenching)[39, 40]. However, the initial-state parton saturation effects are more evident at large rapidity[41, 42], which has been testified by the high rapidity suppression measured in d+Au collisions[43]. But the decreasing of the parton medium density at large rapidity will lead to a smaller jet energy loss, thus, less suppression caused by jet quenching can be expected. Therefore the suppression measured at large rapidity in central Au+Au collisions may be the result of a compromise between initial- and final-state effects[44]. Maybe, the same parton p_{T} spectra at $y=3.2$ with that at $y=0$ used in our work is just a synthetic embodiment of the two effects.

5 Summary

Using the quark combination model, we study the transverse momentum distributions for identified hadrons at different rapidities in central Au+Au collisions at $\sqrt{s_{\mathrm{NN}}}=200$ GeV, incorporating the collective expansion of the hot medium. We use the measured transverse momentum spectra of π^0 and $\mathrm{K}_{\mathrm{s}}^0$ to determine the values of necessary parameters. Firstly we calculate the transverse spectra of identified hadrons and the ratios of protons/antiprotons to pions in a large transverse momentum range at midrapidity. Our model reproduces the data quite well, which suggests that combination scenario may still play an important role in hadronization at high p_{T} up to 12 GeV/c. Using the same transverse momentum spectra for quarks, we further calculate the transverse momentum spectra at various rapidities $y\sim 0,1$, $\eta=2.2$ and $y\approx 3.2$. The results are in good agreement with the data except those for protons and antiprotons at $y\approx 3.2$.

References

1 Blum T et al. Phys. Rev. D, 1995, **51**: 5153
2 Adams J et al (STAR Collaboration). Nucl. Phys. A, 2005, **757**: 102
3 Gyulassy M, McLerran L. Nucl. Phys. A, 2005, **750**: 30
4 Jacobs P, WANG X N. Prog. Part. Nucl. Phys., 2005, **54**: 443
5 Kolb P F, Heinz U W. arXiv:nucl-th/0305084
6 Braun-Munzinger P, Redlich K, Stachel J. arXiv:nucl-th/0304013
7 Rischke D H. Prog. Part. Nucl. Phys., 2004, **52**: 197
8 Hwa R C, YANG C B. Phys. Rev. C, 2004, **67**: 034902
9 Greco V, Ko C M, Levai P. Phys. Rev. Lett., 2003, **90**: 202302
10 Fries R J, Muller B, Nonaka C, Bass S A. Phys. Rev. Lett., 2003, **90**: 202303
11 Voloshin S A. Nucl. Phys. A, 2003, **715**: 379
12 Molnar D, Voloshin S A. Phys. Rev. Lett., 2003, **91**: 092301
13 LIN Z W, Ko C M. Phys. Rev. Lett., 2002, **89**: 202302
14 SHAO F L, YAO T, XIE Q B. Phys. Rev. C, 2007, **75**: 034904
15 SHAO F L, XIE Q B, WANG Q. Phys. Rev. C, 2005, **71**: 044903
16 YAO T, XIE Q B, SHAO F L. Chinese Physics C, 2008, **32**: 356
17 Abelev B I et al (STAR Collaboration). Phys. Rev. Lett., 2006, **97**: 152301
18 Arsene I et al (BRAHMS Collaboration). Phys. Rev. C, 2005, **72**: 014908
19 Arsene I et al (BRAHMS Collaboration). arXiv:nucl-th/0610021.
20 Radoslaw Karabowicz (BRAHMS Collaboration). Nucl. Phys. A, 2006, **774**: 477—480
21 XIE Q B, LIU X M. Phys. Rev. D, 1988, **38**: 2169
22 LIANG Z T, XIE Q B. Phys. Rev. D, 1991, **43**: 751
23 WANG Q, XIE Q B. J. Phys. G, 1995, **21**: 897
24 ZHAO J Q, WANG Q, XIE Q B. Sci. Sin. A, 1995, **38**: 1474
25 WANG Q, SI Z G, XIE Q B. Int. J. Mod. Phys. A, 1996, **11**: 5203
26 SI Z G, XIE Q B, WANG Q. Commun. Theor. Phys., 1997, **28**: 85
27 WANG Q, XIE Q B. Phys. Rev. D, 1995, **52**: 1469
28 WANG Q, XIE Q B, SI Z G. Phys. Lett. B, 1996, **388**: 346
29 WANG Q, Gustafson G, XIE Q B. Phys. Rev. D, 2000, **62**: 054004
30 WANG Q, Gustafson G, JIN Y, XIE Q B. Phys. Rev. D, 2001, **64**: 012006
31 Back B B et al (PHOBOS Collaboration). arXiv:nucl-ex/0301017
32 Sjostrand T et al. Comput. Phys. Commun., 2001, **135**: 238
33 Hofmann M et al. Phys. Lett. B, 2000, **478**: 161
34 Schnedermann E, Sollfrank J, Heinz U. Phys. Rev. C, 1993, **48**: 2462; Schnedermann E, Heinz U. Phys. Rev. C, 1994, **48**: 1675
35 Retiére F et al. nucl-ex/0111013 (2001); Retiére F, Lisa M. Phys. Rev. C, 2004, **70**: 044907
36 Tadaaki Isobe (PHENIX Collaboration). Acta Phys. Hung. A, 2006, **27**: 227—230
37 Greco V, Ko C M, Levai P. Phys. Rev. C, 2003, **68**: 034904
38 Hwa R C, YANG C B. Phys. Rev. C, 2004, **70**: 024905
39 Adler S S et al (PHENIX Collaboration). Phys. Rev. Lett., 2003, **91**: 072303
40 Admas J et al (STAR Collaboration). Phys. Rev. Lett., 2003, **91**: 072304
41 Kharzeev D, Kovchegov Y V, Tuchin K. Phys. Rev. D, 2003, **68**: 094013; Kharzeev D, Levin E, McLerran L. Phys. Lett. B, 2003, **561**: 93
42 Jalilian-Marian J, Nara Y, Venugopalan R. Phys. Lett. B, 2003, **577**: 54; Dumitru A, Jalilian-Marian J. Phys. Rev. Lett., 2002, **89**: 022301
43 Arsene I et al (BRAHMS Collaboration). Phys. Rev. Lett., 2003, **93**: 242303
44 Debbe R (BRAHMS Collaboration). AIP Conf. Proc., 2006, **870**: 707—711